High variability in strain estimation errors when using a commercial ultrasound speckle tracking algorithm on tendon tissue.

Abstract

Background: Ultrasound speckle tracking offers a non-invasive way of studying strain in the free Achilles tendon where no anatomical landmarks are available for tracking. This provides new possibilities for studying injury mechanisms during sport activity and the effects of shoes, orthotic devices and rehabilitation protocols on tendon biomechanics.

Purpose: To investigate the feasibility of using a commercial ultrasound speckle tracking algorithm for assessing strain in tendon tissue.

Material and Methods: A polyvinyl alcohol (PVA) phantom, three porcine tendons and a human Achilles tendon were mounted in a materials testing machine and loaded to 4% peak strain. Ultrasound long-axis cine-loops of the samples were recorded. Speckle tracking analysis of axial strain was performed using a commercial speckle tracking software. Estimated strain was then compared to reference strain known from the materials testing machine. Two frame rates and two region of interest (ROI) sizes were evaluated.

Results: Best agreement between estimated strain and reference strain was found in the PVA phantom (absolute error in peak strain: 0.21 ± 0.08%). The absolute error in peak strain varied between 0.72 ± 0.65% and 10.64 ± 3.40% in the different tendon samples. Strain determined with a frame rate of 39.4 Hz had lower errors than 78.6 Hz as was the case with a 22 mm compared to an 11 mm ROI.

Conclusion: Errors in peak strain estimation showed high variability between tendon samples and were large in relation to strain levels previously described in the Achilles tendon.

Keywords: speckle tracking, strain, Achilles tendon, ultrasound

Introduction

In order to better understand mechanisms of Achilles tendon injury, it is valuable to study how strain in the tendon varies with different exercises and choice of shoes etc. To design improved orthotic devices for treatment of Achilles tendon disease, their biomechanical effects on the tendons need to be investigated. Strain in the Achilles tendon has previously been determined with radiostereometric analysis (RSA) which involves the insertion of tantalum beads into the tendon (1). Ultrasound offers a non-invasive way of studying tendons. Deformation in the Achilles tendon has been calculated using muscle fascicle length and pennation angle in B-mode ultrasound images as model input (2, 3). This method is dependent upon tracking musculotendinous junctions and can therefore not be applied to the distal free Achilles tendon where much of tendon pathology occurs.

Ultrasound speckle tracking is a technique to quantify tissue motion based on tracking of unique patterns created by interference of reflected ultrasound beams in a series of images. It is independent of anatomical landmarks and can therefore be applied to free tendon where much of tendon pathology occurs. A number of ultrasound speckle tracking algorithms, both in-house developed (4-6) and commercially available (7) have been validated for assessment of displacement in tendons. It would be desirable to measure strain rather than displacement in tendons as strain is more likely to be a cause of injury. Assessing strain instead of displacement has been described as more challenging as it requires tracking of differences in displacements within a region (8). Commercially available speckle tracking algorithms originally developed for the myocardium have previously been used to study strain in tendons (9), although they were designed for a speckle and motion pattern different from that of tendons. As tendons move along the body surface, relevant measurements must be made perpendicular to the ultrasound beam and therefore depend on the lateral resolution of the

image, which is intrinsically lower than the axial resolution. Strain in the Achilles tendon during walking (2, 10) can be expected to be lower than that described in the myocardium (11). This places higher demands on measurement accuracy.

For the above reasons, algorithms originally developed for assessment of strain in the myocardium may not be accurate in assessing strain in tendons. However, as these algorithms are commercially available to clinicians it would be valuable to investigate if they can be accurately applied to tendons. The aim of this study was to investigate the feasibility of a commercial ultrasound speckle tracking algorithm for assessing strain in tendon tissue, including the human Achilles tendon, in an in-vitro experimental setup.

Material and Methods

A polyvinyl alcohol (PVA) phantom, three porcine flexor digitorum tendons and a human Achilles tendon allograft were successively mounted in a materials testing machine (ElectroPuls E3000, Instron, Norwood, MA, USA) and subjected to a strain protocol. Ultrasound long-axis cine-loops of the tendons were recorded and speckle tracking analysis of strain was performed (Fig. 1). Estimated strain was then compared to the reference strain known from the materials testing machine.

Experimental setup

A PVA phantom with dimensions similar to the human Achilles tendon (115x15x5 mm) was constructed. It was molded from 82% H_2O, 15% PVA (Sigma-Aldrich, St Louis, MO, USA) and 3% graphite powder (Merck, Darmstadt, Germany) by weight, and then frozen and thawed for three cycles (20h at -20^{0}C / 20h at 20^{0}C). The PVA phantom had flanges that were

mounted in plastic attachments in the materials testing machine (Fig. 1a). The flexor digitorum tendons with attached distal phalanx were removed from fresh frozen porcine feet. The proximal end was attached using a pressure clamp and the distal bony end was molded in a fiberglass block and screwed into the center of the materials testing machine. A human Achilles tendon allograft with calcaneal bone was obtained from a patient undergoing subacute lower leg amputation due to ischemia. The tendon was frozen directly after harvesting and then thawed before testing. It was mounted in the materials testing machine as described above (Fig. 1b). Before commencing the test procedure the initial PVA phantom or tendon length was measured using vernier calipers.

The materials testing machine was programmed to strain the PVA phantom or tendon in a manner mimicking physiological tendon motion. To obtain input data an ultrasound acquisition (Vivid7, 12L linear array transducer, GE Healthcare, Horten, Norway) of the Achilles tendon of a healthy male walking on a treadmill at 2 km/h was made. Strain in the Achilles tendon was assessed from the ultrasound loops using EchoPAC 110.1.2 (GE Healthcare) and data averaged from three consecutive strides was used. The reference curve for each PVA phantom or tendon sample and trial was obtained from displacement data provided by a sensor on the motor shaft of the materials testing machine. The observed displacement was divided by the initial length of the PVA phantom or tendon to find the reference value of strain $\varepsilon(t)$ (Figs. 2-4).

Fresh frozen porcine feet were purchased at the local food store. The Stockholm regional ethical committee approved the study and the patient providing the Achilles tendon allograft gave written informed consent.

Image acquisition

An 8L-RS linear array transducer (GE Healthcare) connected to a Vivid*i* ultrasound machine (GE Healthcare) was placed on the PVA phantom or tendon. For the tendon samples, a 4 mm thick acoustic stand-off pad (Civco, Kalona, IA, USA) covered with ultrasound gel was placed between the ultrasound probe and the tendon. For the PVA phantom the ultrasound probe was only covered with gel. To minimize the risk of reverberation artefacts a block of ultrasound absorbent material with an uneven surface covered with gel was placed behind the PVA phantom or tendon (Fig. 1). Two different frame rates were evaluated: frame rate 39.4 Hz with default center frequency 13 MHz and frame rate 78.6 Hz with default center frequency 10 MHz. The programmed motion was performed ten times per sample and frame rate setting (depth: 3 cm, one focus point in the center of the PVA phantom or tendon).

Speckle tracking

EchoPAC 110.1.2, 2D strain (GE Healthcare) was used to assess strain. For each ultrasound acquisition, the frames in which the motion occurred were manually chosen for analysis. Two different region of interest (ROI) sizes were tested; 22mm and 11mm. As the lower frame rate (39.4 Hz) gave more accurate strain values in the tendon samples, this frame rate was chosen for evaluating the two different ROI sizes. The ROI's were placed in the tendon along the border facing the ultrasound transducer (Fig. 5). The EchoPAC software has an in-built function which suggests whether or not to accept strain trials based on an assessment of tracking quality. The software automatically divided the ROI into three segments and evaluated tracking quality for each segment. A ROI was accepted if visual assessment indicated that it followed the underlying speckle pattern and if tracking for all segments was deemed valid by the software control. Global strain data with drift compensation and the

default setting for temporal and spatial smoothing were saved in text format. The EchoPAC drift compensation function was applied to ensure that strain always returned to zero at the end of each trial.

Strain analysis

Mean strain curves over the ten cycles with standard deviations were calculated in Matlab R2012b (Mathworks Inc, Natick, MA, USA). Root mean square errors (RMSE) were calculated for all strain curves using Matlab according to:

$$RMSE = \sqrt{\sum_{t=1}^{N} \frac{(\varepsilon(t) - \hat{\varepsilon}(t))^2}{N}}$$

where $\hat{\varepsilon}(t)$ was estimated strain, $\varepsilon(t)$ reference strain and N the number of frames in one motion cycle. Strain data were imported into Origin 8 (Microcal Inc, Northampton, MA, USA) and the strain peak corresponding in time with the reference peak strain was manually identified for each trial. The peak strain values ($\hat{\varepsilon}_{peak}(\mathrm{t})$) were compared to the corresponding reference peak strain (ε_{peak}) and means and standard deviations of the absolute errors ($|\hat{\varepsilon}_{peak} - \varepsilon_{peak}|$) were calculated for each tendon for the ten repeated measurements. Frame rate 39.4 Hz and ROI size 22 mm resulted in lower RMSE's and peak strain values and errors are therefore presented for these settings.

Results

The RMSE of the estimated strain curves for the PVA phantom, the porcine tendons and the human Achilles tendon allograft for the two different frame rates and ROI sizes are shown in Table 1. It was difficult to achieve acceptable tracking using the 11 mm ROI and tracking

quality was deemed invalid in several cycles on porcine tendon 2 and 3 despite repeated attempts to place a ROI (Table 2). Mean strain curves of ten repeated cycles with standard deviations for the PVA phantom, the porcine tendons and the human Achilles tendon allograft (frame rate 39.4 Hz, 22 mm ROI) are shown in Figs. 2-4. Estimated peak strains and absolute errors of peak strain are shown in Table 2. Best agreement between estimated strain and reference strain was found in the PVA phantom, with an absolute error in peak strain of 0.25 ± 0.05%. High variations in absolute error of peak strain and RMSE were observed when estimating strain in the tendon samples. The absolute error in peak strain varied between 0.72 ± 0.65% and 14.85 ± 3.96% in the tendons.

Discussion

A non-invasive method for studying strain in the free Achilles tendon where no anatomical landmarks are available for tracking would facilitate analysis of injury mechanisms during sport activity and the effects of shoes, orthotic devices and rehabilitation protocols on tendon biomechanics. In this study a commercial ultrasound speckle tracking algorithm was evaluated for assessing strain in tendons in an in-vitro experimental setup.

There were considerable variations in the performance of the tested algorithm between different tendon samples, frame rates and ROI sizes. The RMSE's for the tendon samples (porcine tendon 2, porcine tendon 3 and the human tendon allograft) were significantly ($p < 0.01$) lower when the lower frame rate (39.4 Hz) was used. Although a higher frame rate provides greater temporal resolution, it may be unfavorable in speckle tracking as it could result in sub-pixel motion if tissue motion between frames is not at least one pixel. In two

previous studies using EchoPAC to assess motion in in-vivo tendons a higher frame rate (72-79 Hz) was used (9, 12). Chernak et al. observed that the normalized cross-correlations of kernels was reduced slightly when the frame rate was lowered from 63 Hz to 33.5 Hz, but that cumulative tracking results were largely unaffected (4).

The 22 mm ROI was the largest ROI possible without the ROI moving out of the visible tendon image. A ROI half this size was also chosen for testing. The 22 mm ROI was significantly more accurate than the 11 mm ROI with lower RMSE in porcine tendon 1 ($p<0.01$) and in the human tendon allograft ($p=0.02$). It was also observed that it was easier to achieve tracking that was deemed valid by the software when using the larger ROI. The better performance with the larger ROI was presumably an effect of a strain estimation based on a larger amount of motion estimations within the ROI.

Using the frame rate and ROI size that were found to work best (39.4Hz, 22 mm), the strain estimation errors still showed large variation between the different tendons. The RMSE's ranged from 1.19 ± 0.12% to 10.64 ± 3.40%. Large variations in tendon strain have previously been observed in-vivo when using commercial speckle tracking software. In a recent study, strain in the deep portion of the supraspinatus tendon was reported to vary between 1.59% and 28.88% in 15 subjects during active isotonic elevation of the arm (9). However, the validity and reproducibility was not evaluated in this study. Peak strain in the Achilles tendon during walking can be expected to be approximately 5% (2, 10). In the present study, a peak strain of approximately 4% was used. Absolute errors in peak strain in the tendons ranged between 0.72 ± 0.65% and 14.85 ± 3.96%. These errors are high in relation to physiological strain observed in Achilles tendons in-vivo.

Although speckle tracking assessment of displacement has been suggested to be less challenging than strain assessment in tendons, reported errors of tendon displacement are diverging. Korstanje et al. successfully validated an in-house speckle tracking algorithm for assessment of displacement in human flexor digitorum (FD) tendons and the relative error was found to be 1.6% (5). Yoshii et al. used another commercial speckle tracking software (Syngo VVI software, Siemens Medical Solutions Inc., Malvern, PA, USA) to estimate displacement in FD tendons and validated it against displacement calculated from changes in finger joint angles. The excursions from the speckle tracking measurements were underestimated and the mean absolute error was reported to be about 1.1 cm when estimating excursions of approximately 1.0 - 2.5 cm (7). Chernak et al. evaluated ultrasound elastography for assessment of displacement in porcine flexor tendons and showed that elastography consistently underestimated displacement with considerable variations between samples, although correlations between estimated displacement and reference displacement were high (4).

The superior performance of the algorithm on the PVA phantom (Table 2) presumably has a number of explanations. Strain estimation in tendons is dependent on the lateral resolution of the ultrasound beam which is lower than the axial resolution. This did not seem to have a major influence on the accuracy of strain estimation in the PVA phantom where the speckles were small, distinct and evenly distributed. However, lateral tracking would be expected to be more challenging in tendon tissue due to its striated appearance. The tendons may not have followed the motion of the materials testing machine during rapid changes in strain as accurately as the PVA phantom. This may have been due to the velocity of the material

testing machine momentarily being greater than the shortening velocity of the tendon. The input velocity in this experiment was based on velocities found during walking and this phenomenon may be similar to the action of the in-vivo Achilles tendon reported by Komi (13). Displacement within the Achilles tendon is inhomogeneous from superficial to deep (12, 14) so it is quite likely that tendon tissue may also have regional differences in elastic properties along the length of the tendon. Such inhomogeneity along the length of the tendon may lead to local differences in strain, which were presumably avoided in the homogenous PVA phantom. However, care was taken to maintain the same position of the ultrasound probe relative to the tendon between trials, so inhomogeneity of the tendon along its length should not be the reason for large intra-tendon variability of strain. Similarly helical twisting of the tendon may lead to different strain results if speckle tracking is applied at different heights or depths.

It was observed that it was more difficult to achieve acceptable tracking quality on porcine tendon 2 and 3 as compared to porcine tendon 1 (Fig. 3) and there was also a larger variation in strain estimates between trials in porcine tendon 2 and 3. A possible explanation for the large difference in absolute errors of peak strain between the porcine tendons is that the speckle tracking software is sensitive to the speckle pattern to be tracked and that the tendons included in the study had slightly different speckle patterns. All tendons were fresh frozen and thawed before use and mounted into the materials testing machine according to the same protocol and no damage to the tendons was apparent that would explain differences in tracking errors but small differences in experimental set up may have affected the results.

There are limitations of the methods used in this study. Tendons have a striated speckle pattern and for this reason Korstanje et al. suggests the use of elongated kernels (5). A limitation of the commercial speckle tracking software used in this study is that it is not possible for the user to know or adapt the kernel size. An oblique pull on the tendon may have occurred if the bony attachment was not optimally centered in the materials testing machine, while the PVA phantom was molded with flanges that fitted into plastic attachments screwed into the materials testing machine assuring that it was centered at both top and bottom. This in turn might have resulted in out of plane motion of speckles which is a known source of error in speckle tracking (7). Minimal changes in probe position may have occurred due to the tendon material slipping in the gripping device. Furthermore, reflection artefacts may have affected the performance of the speckle tracking algorithm.

Porcine flexor digitorum tendons have a speckle pattern in ultrasound images similar to human tendons. The amount of strain and the strain rate applied to the tendons were similar to those in the human Achilles tendon during walking so speckle displacement and velocities in this study were assumed to be physiological. Tendons often run close to the body surface so the measurement depth in this study was similar to clinical measurements. It therefore seems appropriate to extrapolate the presented data to clinical applications.

In conclusion, errors in peak strain estimation showed a high variability between tendon samples. Absolute errors of up to 14.85% were described, which is high when compared to the strain previously described in the Achilles tendon during normal walking. Strain estimation in tendon tissue using EchoPAC 2D strain was improved using frame rate 39.4 Hz as compared to 78.6 Hz and a 22 mm ROI resulted in more accurate tracking than an 11 mm

ROI. Validity testing of ultrasound speckle tracking algorithms is imperative prior to application on tendon tissue.

References

1. Schepull T, Kvist J, Andersson C, et al. Mechanical properties during healing of Achilles tendon ruptures to predict final outcome: a pilot Roentgen stereophotogrammetric analysis in 10 patients. BMC Musculoskelet Disord 2007;8:116.

2. Ishikawa M, Komi PV, Grey MJ, et al. Muscle-tendon interaction and elastic energy usage in human walking. J Appl Physiol 2005;99:603-608.

3. Lichtwark GA, Wilson AM. In vivo mechanical properties of the human Achilles tendon during one-legged hopping. J Exp Biol 2005;208:4715-4725.

4. Chernak LA, Thelen DG. Tendon motion and strain patterns evaluated with two-dimensional ultrasound elastography. J Biomech 2012;45:2618-2623.

5. Korstanje JW, Selles RW, Stam HJ, et al. Development and validation of ultrasound speckle tracking to quantify tendon displacement. J Biomech 2010;43:1373-1379.

6. Pearson SJ, Ritchings T, Mohamed AS. The use of normalized cross-correlation analysis for automatic tendon excursion measurement in dynamic ultrasound imaging. J Appl Biomech 2013;29:165-173.

7. Yoshii Y, Villarraga HR, Henderson J, et al. Speckle tracking ultrasound for assessment of the relative motion of flexor tendon and subsynovial connective tissue in the human carpal tunnel. Ultrasound Med Biol 2009:35;1973-1981.

8. Slagmolen P, Scheys L, D'Hooge J, et al. In regard to: "In vivo strain analysis of the intact supraspinatus tendon by ultrasound speckles tracking imaging" . J Orthop Res 2011; 29:1931-1937. J Orthop Res 2012;30:2054-2056; author reply 6-7.

9. Kim YS, Kim JM, Bigliani LU, et al. In vivo strain analysis of the intact supraspinatus tendon by ultrasound speckles tracking imaging. J Orthop Res 2011;29:1931-1937.

10. Lichtwark GA, Wilson AM. Interactions between the human gastrocnemius muscle and the Achilles tendon during incline, level and decline locomotion. J Exp Biol 2006;209:4379-4388.

11.;Reckefuss N, Butz T, Horstkotte D, et al. Evaluation of longitudinal and radial left ventricular function by two-dimensional speckle-tracking echocardiography in a large cohort of normal probands. Int J Cardiovasc Imaging 2011;27:515-526.

12. Arndt A, Bengtsson AS, Peolsson M, et al. Non-uniform displacement within the Achilles tendon during passive ankle joint motion. Knee Surg Sports Traumatol Arthrosc 2012;20:1868-1874.

13. Komi PV. Relevance of in vivo force measurements to human biomechanics. J Biomech 1990;23:23-34.

14. Slane LC, Thelen DG. Non-uniform displacements within the Achilles tendon observed during passive and eccentric loading. J Biomech 2014;47:2831-2835.

Table 1. RMSE of the estimated strain curves

	RMSE 22 MM ROI 39.4 HZ	RMSE 22 MM ROI 78.6 HZ	RMSE 11 MM ROI 39.4 HZ	P-VALUE 39.4 HZ VS 78.6 HZ	P-VALUE 22 MM VS 11 MM ROI
PVA phantom	0.21 ± 0.08	0.14 ± 0.05	0.21 ± 0.09	0.03	0.79
porcine tendon 1	1.36 ± 0.40	-	1.93 ± 0.48	-	< 0.01
porcine tendon 2	10.64 ± 3.40	18.36 ± 1.03	8.44 ± 6.11 **	< 0.01	0.34
porcine tendon 3	1.85 ± 0.76 *	4.25 ± 1.45	8.83 ± 0.07 ***	< 0.01	NA
human allograft	1.19 ± 0.12	1.97 ± 0.13	1.49 ± 0.32	< 0.01	0.02

RMSE of the estimated strain curves for the PVA phantom, the porcine tendons and the human Achilles tendon allograft for frame rates 39.4 Hz and 78.6 Hz using a 22 mm ROI and for 39.4 Hz using an 11 mm ROI. *n=8, **n=9, ***n=2, NA: not calculated due to low n. For porcine tendon 1 only frame rate 39.4 Hz was available for analysis due to technical problems.

Table 2. Peak strain estimation results

	ESTIMATED PEAK STRAIN MEAN ± SD (%)	REFERENCE PEAK STRAIN MEAN ± SD (%)	ABSOLUTE ERROR PEAK STRAIN MEAN ± SD (%)
PVA PHANTOM	4.32 ± 0.05	4.07 ± 0.00	0.25 ± 0.05
PORCINE TENDON 1	6.01 ± 0.59	4.41 ± 0.00	1.60 ± 0.59
PORCINE TENDON 2	18.96 ±3.95	4.12 ± 0.02	14.85 ± 3.96
PORCINE TENDON 3*	4.20 ± 1.33	4.16 ± 0.01	0.96 ± 0.86
HUMAN ALLOGRAFT	3.77 ± 0.89	4.19 ± 0.01	0.72 ± 0.65

Mean ± standard deviation of estimated peak strain, reference peak strain and absolute error $\left(\left|\hat{\varepsilon}_{peak} - \varepsilon_{peak}\right|\right)$ of peak strain in the polyvinyl alcohol (PVA) phantom and ex-vivo tendons (39.4 Hz and 22 mm ROI). * n=8

Figures:

Figure 1:

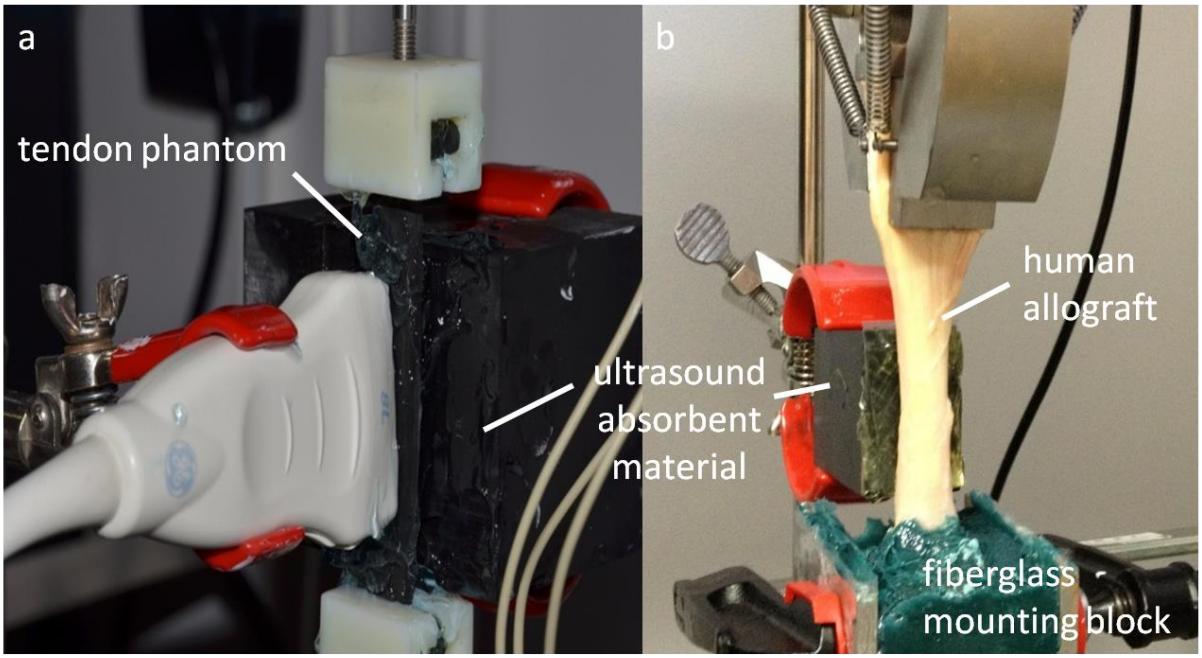

Fig. 1 a) Polyvinyl alcohol phantom mounted in the materials testing machine with the ultrasound transducer in front. b) Human tendon allograft mounted in the materials testing machine.

Figure 2:

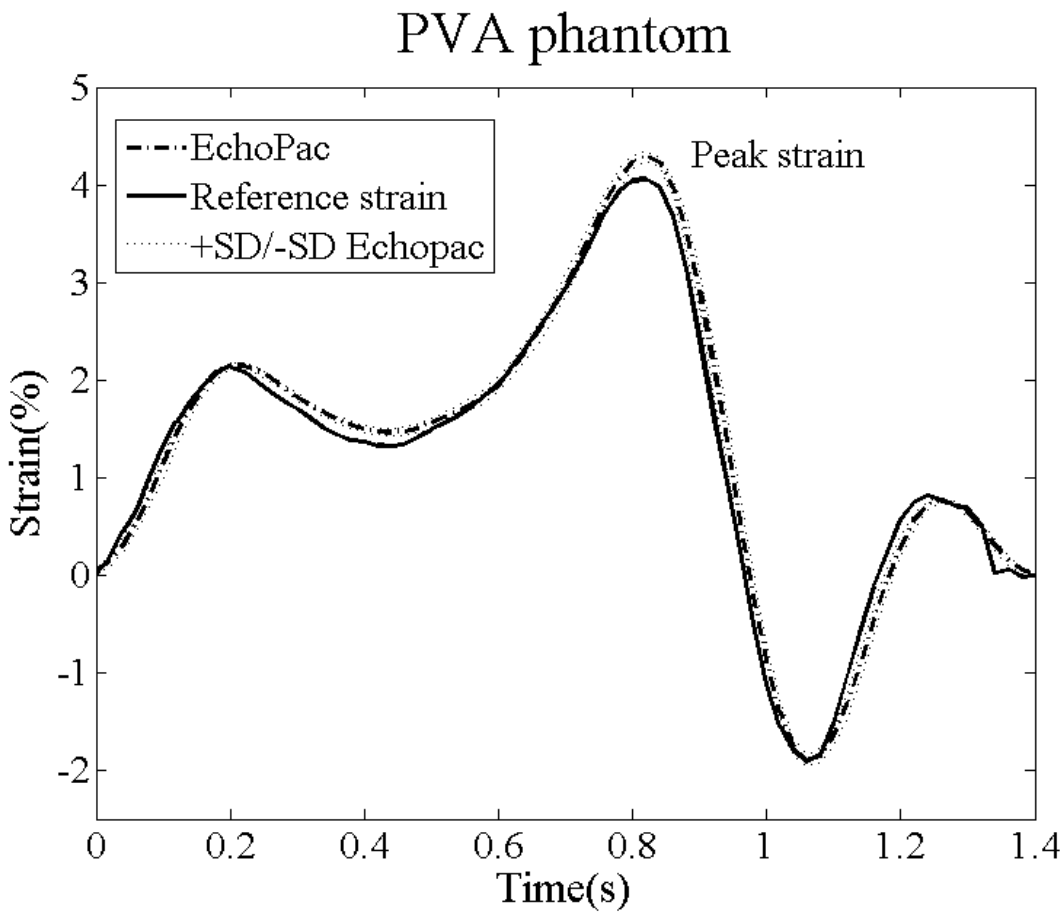

Fig. 2: Reference strain and mean strain curves with standard deviations (SD) for the polyvinyl alcohol phantom using frame rate 39.4 Hz and a 22 mm ROI.

Figure 3:

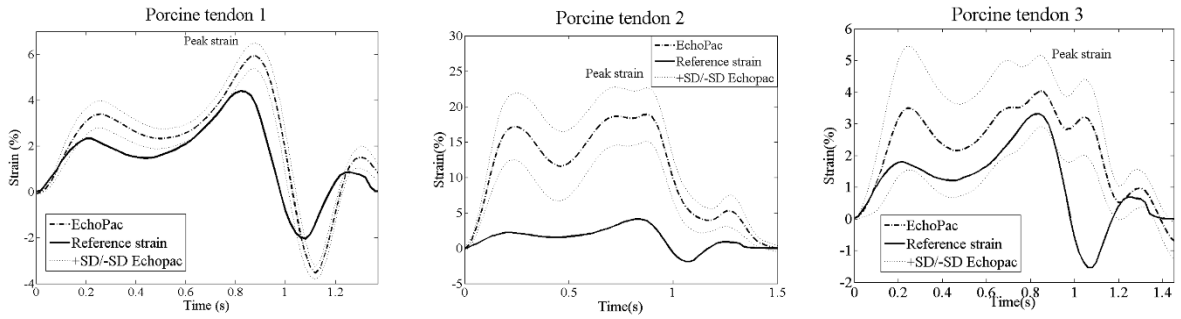

Fig. 3: Reference strain and mean strain curves with standard deviations (SD) for porcine tendon 1, porcine tendon 2 and porcine tendon 3 using frame rate 39.4 Hz and a 22 mm ROI.

Figure 4:

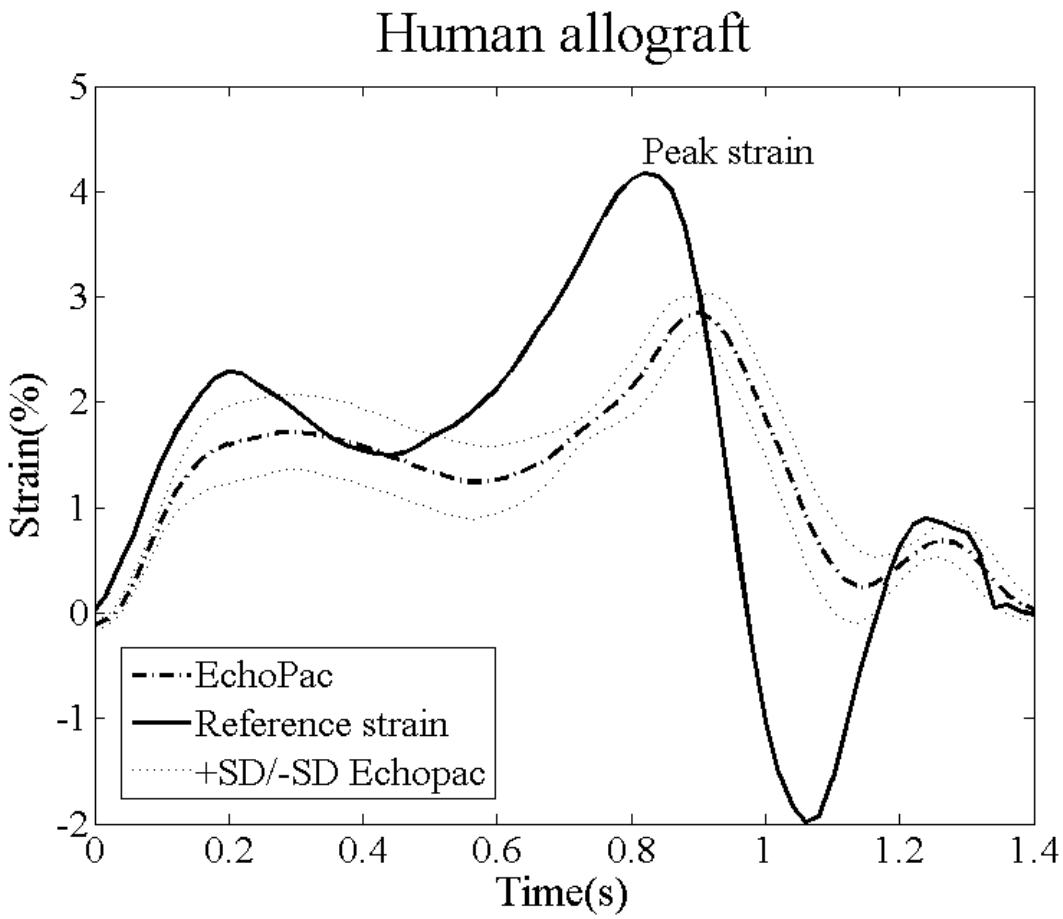

Fig. 4: Reference strain and mean strain curves with standard deviations (SD) for the human tendon allograft using frame rate 39.4 Hz and a 22 mm ROI.

Figure 5:

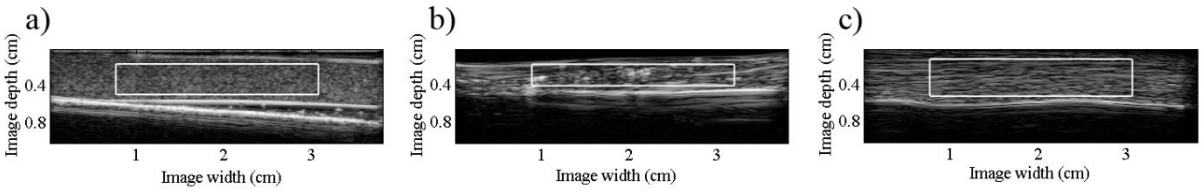

Fig. 5: Example of a 22 mm region of interest (ROI) placed in a) the polyvinyl alcohol phantom, b) a porcine tendon and c) the human tendon allograft. The transducer is placed against the upper surface seen in the pictures.